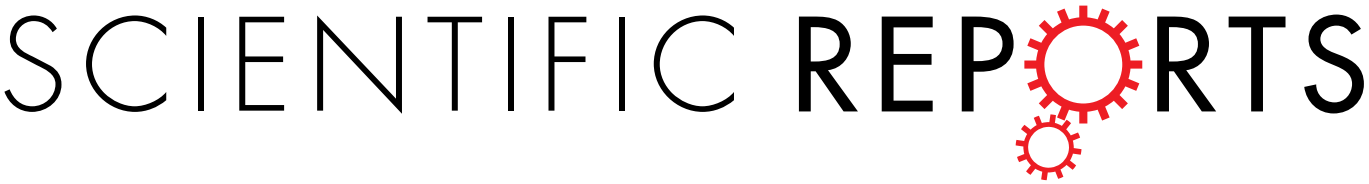

OPEN

Probe Into the Influence of Crosslinking on CO_2 Permeation of Membranes

Received: 10 October 2016
Accepted: 30 November 2016
Published: 04 January 2017

Jinghui Li[1], Zhuo Chen[1], Ahmad Umar[2], Yang Liu[3], Ying Shang[1], Xiaokai Zhang[1] & Yao Wang[1]

Crosslinking is an effective way to fabricate high-selective CO_2 separation membranes because of its unique crosslinking framework. Thus, it is essentially significant to study the influence of crosslinking degree on the permeation selectivities of CO_2. Herein, we report a successful and facile synthesis of a series of polyethylene oxide (PEO)-based diblock copolymers (BCP) incorporated with an unique UV-crosslinkable chalcone unit using Reversible Addition-Fragmentation Chain Transfer Polymerization (RAFT) process. The membranes of as-prepared BCPs show superior carbon dioxide (CO_2) separation properties as compared to nitrogen (N_2) after UV-crosslinking. Importantly, the influence of different proportions of crosslinked chalcone on CO_2 selectivities was systematically investigated, which revealed that CO_2 selectivities increased obviously with the enhancement of chalcone fractions within a certain limit. Further, the CO_2 selectivities of block copolymer with the best block proportion was studied by varying the crosslinking time which confirmed that the high crosslinking degree exhibited a better CO_2/N_2 ($\alpha_{CO2/N2}$) selectivities. A possible mechanism model revealing that the crosslinking degree played a key role in the gas separation process was also proposed.

The deteriorating environment caused by the global warming has become an immediate threat nowadays. Even though the excessive release of CO_2 is considered as a real threat for the global warming it is also regarded as a new energy resource which is attracting much attention nowadays. The conventional techniques for capturing CO_2 include "wet scrubbing" using alkaline solutions and membrane separation. However, "wet scrubbing" and traditional membrane separation process possess some drawbacks which include high cost, erosion of equipment and irreversible process[1–4]. Recently, fabrication of CO_2-responsive materials is regarded as a new approach to solve such drawbacks[2–6]. Meanwhile, invention of novel membrane separation technology has always attracted great interests in CO_2 capture from economic and environmental points of view due to its various advantages such as low energy cost, high-efficiency, high-stability, ease of fabrication[7–15]. Literature reveals, according to the theory of gas separation, that there are several kinds of membranes including inorganic membranes[16], polymeric membranes[17–25] and facilitated membranes[26–28] which are used for CO_2 capture[29].

It was observed that the polymers containing EO (ethylene oxide) units were widely used in the separation of CO_2 from other gases[30–36]. It was found that EO units showed strong interactions with CO_2 compared with other gases such as N_2, CH_4, H_2, especially with the temperature increased, EO units became more favored to CO_2, which resulted in high CO_2 permeabilities and selectivities over other gases[37]. A high content of EO segments was supposed to lead high CO_2 permeabilities according to the reported principles[38], however, it was explored that the PEO chains with high molecule weight was easy to crystallize, resulting in the decrease of the chain mobility, and hence exhibiting a reduction in the CO_2 permeabilities and selectivities. Therefore, in order to avoid such crystallization, several methods were proposed, such as mixing the liquid PEO with rigid polymers[39], doping PPO[40], building a network by crosslinking PEO[37,41–47] and so on. The influence of crosslinking on gas permeation has always been the issues researchers concerned about. Lin *et al.* have studied the effect of crosslinking on gas permeabilities in crosslinked Poly(Ethylene Glycol) Diacrylate, notably, they found that crosslinking had negligible effect on the gas separation properties of Poly(Ethylene Glycol) Diacrylate[39]. However, Our previous

[1]School of Chemistry and Environment, Key Laboratory of Bio-Inspired Smart Interfacial Science and Technology of Ministry of Education, Beihang University, Beijing 100191, PR China. [2]Department of Chemistry, Faculty of Science and Arts and Promising Centre for Sensors and Electronic Devices (PCSED), Najran University, Najran 11001, Kingdom of Saudi Arabia. [3]Beijing Key Laboratory of Radiation Advanced Materials, Beijing Research Center for Radiation Application, Beijing 100015, China. Correspondence and requests for materials should be addressed to Y.W. (email: yao@buaa.edu.cn)

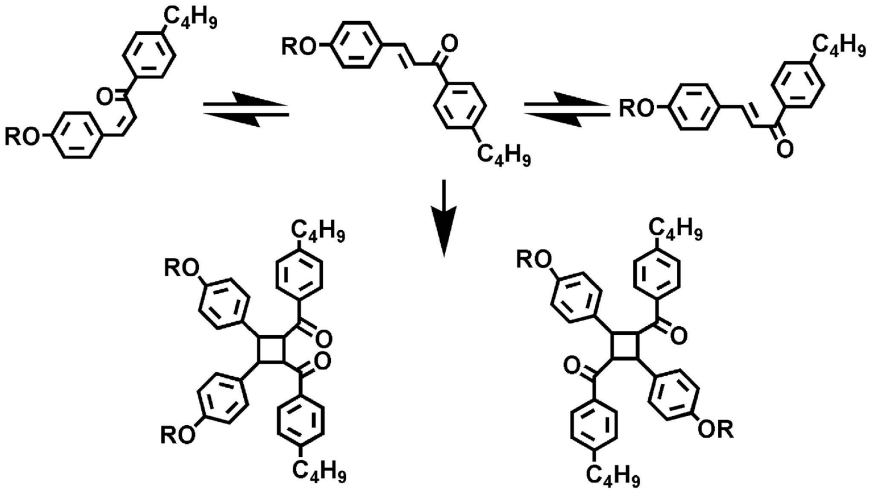

Figure 1. Photochemical Reaction of the chalcone under UV irradiation forming "Head to Head" and "Head to Tail" structures[49].

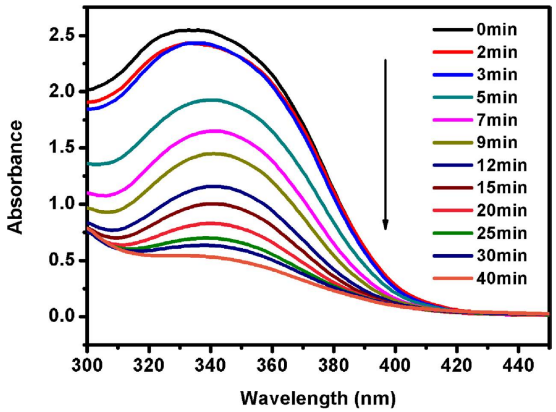

Figure 2. Photoreactions of the block copolymers with irradiation at 365 nm.

work reported that a kind of CO_2-selective membrane consisting of EO segments and commercially available UV-crosslinker coumarin achieved high CO_2 selectivities compared with N_2 and He after UV-crosslinking, which suggested that the impact of crosslinking on gas permeation properties existed[48]. Based on this, it is our motivation in this work to have an insight on the role of crosslinking degree during the gas separation process of PEO-based membranes.

Chalcone was chosen by Iyoda and his coworkers as an UV-crosslinker to better control the crosslinking degree in their previous work[49,50]. It was because that the chalcone could be crosslinked like "head to head" and "head to tail" and hence forming a higher crosslinking degree of membrane structure as shown in Fig. 1. Therefore, in this work, in order to better understand the correlation of crosslinking degree and CO_2 permeation properties, chalcone was selected as a unique crosslinkable segment instead of coumarin. In detail, chalcone was designed as a UV-crosslinker to study the regulation of gas permeation and crosslinking degree. For this, firstly, the chalcone segments and EO units were synthesized. Further, a series of block copolymers consisting of PEO (poly(ethylene oxide)) and PMA (poly(methacrylate) with chalcone mesogens) with different block ratios (PEO_{11}-*b*-PMA(rChal)$_7$, PEO_{11}-*b*-PMA(rChal)$_9$, PEO_{11}-*b*-PMA(rChal)$_{12}$, PEO_{11}-*b*-PMA(rChal)$_{16}$) were fabricated using Reversible Addition-Fragmentation Chain Transfer Polymerization (RAFT) method. The prepared copolymers were further investigated to examine the changes of gas permeabilities and selectivities of the membranes before and after UV crosslinking, respectively. Moreover, the variations of gas permeabilities and selectivities by changing the fraction of the crosslinkable block and crosslinking time were discussed. Based on the obtained results, a plausible mechanism between crosslinking degree and CO_2 permeation properties was also demonstrated.

Results and Discussion

Characterizations of crosslinking degree. The effect of UV-crosslinking time on the prepared membranes was examined by UV-vis absorption spectroscopy. Figure 2 exhibited the typical UV-Vis spectra of the prepared membrane UV-crosslinking for various time intervals. The UV-Vis spectral trend was monitored at

Temp (°C)	Condition	N_2 Permeabilities (barrer)	CO_2 Permeabilities (barrer)	$\alpha_{(CO2/N2)}$
30	Un-crosslinked	84.40	138.01	1.63
	Crosslinked	38.71	113.18	2.92
40	Un-crosslinked	85.16	178.91	2.10
	Crosslinked	31.79	155.30	4.89
50	Un-crosslinked	88.01	229.14	2.61
	Crosslinked	20.97	217.29	10.36
60	Un-crosslinked	90.67	250.46	2.76
	Crosslinked	19.89	249.87	12.56

Table 1. Pure Gas Permeabilities and Selectivities of PEO-*b*-PMA (rChal) (11:7) Un-crosslinked Compared with Crosslinked Membrane. Permeances at 1×10^6 ($cm \cdot s^{-1} \cdot cmHg^{-1}$), were calculated by dividing the observed flow rate by the area of the membrane (2.84 cm^2) and the pressure gradient (10 psi) employed, using porous Al_2O_3 membrane supports. The values were obtained from 10 independent measurements and the mean value and standard deviations were determined. The error in each case was <5%. The membrane PEO-*b*-PMA (rChal) showed no difference of gas permeation in humid environment.

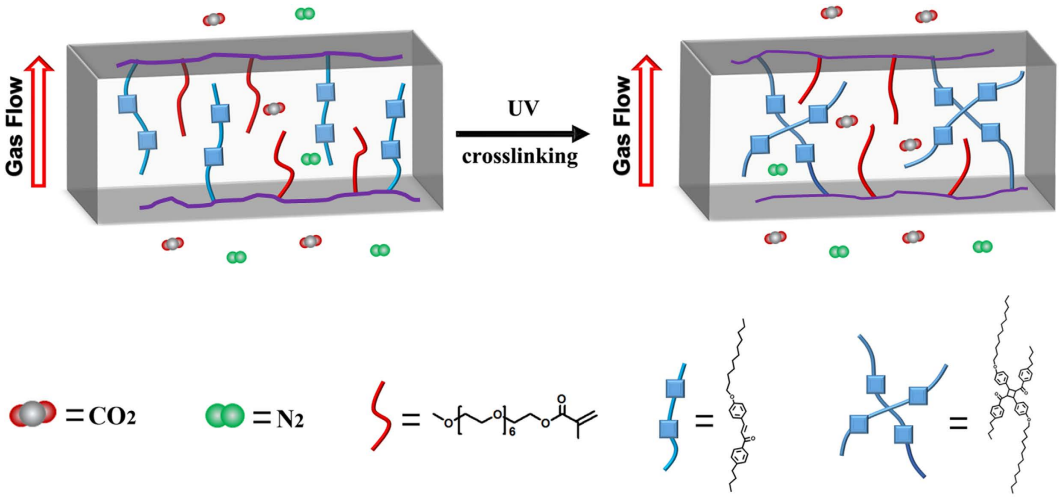

Figure 3. Graphical explanation of PEO-*b*-PMA(rChal) diblock copolymer thin film and CO_2 separation from N_2 gases (CO_2/N_2).

special chalcone absorption band appearing in the range of 300 to 450 nm. The observed UV-vis absorption spectroscopy revealed that the π-π* transition of the chalcone unit had a decrease from the 340 nm absorption band. The observed photoreaction could be explained according to the dimerization of the chalcone moieties through the [2 + 2] cyclization of the double bond[51]. Interestingly, it was observed that with increasing the UV-crosslinking time, the change of absorption spectra tended to balance, which illustrated that the greatest degree of crosslinking reached at 40 min.

Comparison of CO_2 permeation properties of the membranes before and after crosslinking. Table 1 showed the gases permeation and CO_2/N_2 selectivities of the un-crosslinked film compared with crosslinked film with PEO_{11}-*b*-$PMA(rChal)_7$ at different temperature. The $\alpha_{CO2/N2}$ data for other films are demonstrated in Tables S1 and S2. As shown in Table 1, the $\alpha_{CO2/N2}$ of these two membranes were increasing with rising the temperature. Interestingly, $\alpha_{CO2/N2}$ of un-crosslinked membrane was 2.76 at 60 °C which was much smaller than $\alpha_{CO2/N2}$ of crosslinked membrane equal to 12.56. (Figure S1) The selectivities was mainly related to solubility selectivities and diffusivity selectivities which mainly depended on the interactions of EO unit with CO_2 and the free volume of EO, respectively. To explain this phenomenon, a probable mechanism model was proposed to interpret the increase of $\alpha_{CO2/N2}$ (Fig. 3). For un-crosslinked membrane, the EO units and the chalcone units had a large excess free volume and increased the mobility of the chain with the temperature rising, which led to higher gas permeabilities. Notably, differed from N_2, the CO_2 had a strong interaction with EO units, causing the PEO chains more flexible, which also contributed to the final $\alpha_{CO2/N2}$. Referred to crosslinked membrane, for the diffusivity selectivities, crosslinking structure limited the free volume and hence the EO units were confined in the hard regions of crosslinked chalcone walls. With increasing the temperature, the crosslinked hard regions were hardly moved but EO units were more flexible in the limited domain. However, for N_2, the flexible EO units would lead to denser barriers in a limited area[48], and then the less N_2 molecules went through the free volume which produced a low gas permeabilities for N_2. For CO_2, the interactions between EO units and CO_2 increased with rising

Temp. (°C)	Block ratio (PEO:PMA)	N_2 Permeabilities (barrer)	CO_2 Permeabilities (barrer)	$\alpha_{(CO2/N2)}$
30	11:7	38.71	113.18	2.92
	11:9	32.43	108.65	3.35
	11:12	29.05	100.53	3.46
	11:16	26.13	72.62	2.78
40	11:7	31.79	155.30	4.89
	11:9	28.42	142.34	5.01
	11:12	21.40	123.35	5.76
	11:16	19.23	89.43	4.65
50	11:7	20.97	217.29	10.36
	11:9	17.01	216.41	12.72
	11:12	12.64	164.82	13.04
	11:16	11.15	106.71	9.57
60	11:7	19.89	249.87	12.56
	11:9	15.49	219.94	14.20
	11:12	11.19	165.69	14.79
	11:16	10.56	106.99	10.13

Table 2. Pure Gas Permeabilities and Selectivities of Different Block Ratio PEO-*b*-PMA (rChal) Crosslinked Membrane. Permeances at 1×10^6 ($cm \cdot s^{-1} \cdot cmHg^{-1}$), were calculated by dividing the observed flow rate by the area of the membrane (2.84 cm^2) and the pressure gradient (10 psi) employed, using porous Al_2O_3 membrane supports. The values were obtained from 10 independent measurements and the mean value and standard deviations were determined. The error in each case was <5%. The membrane PEO-*b*-PMA (rChal) showed no difference of gas permeation in humid environment.

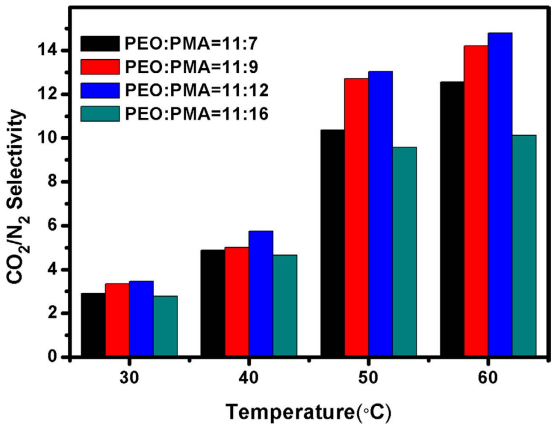

Figure 4. $\alpha_{CO2/N2}$ with PEO:PMA = 11:7(black), 11:9(red), 11:12(blue) and 11:16(green) at different temperature.

the temperature and plasticized EO regions which lead to more flexible EO fraction, thus further increasing the CO_2 permeabilities[52]. Therefore, with such aforementioned discussion, it can be concluded that the crosslinked membranes showed a favored gas selectivities towards CO_2 with increasing the temperature.

Comparison of gas permeation properties of the membranes composed of various block ratio. In this study, four kinds of block copolymers with different block ratios, i.e. PEO_{11}-*b*-$PMA(rChal)_7$, PEO_{11}-*b*-$PMA(rChal)_9$, PEO_{11}-*b*-$PMA(rChal)_{12}$, PEO_{11}-*b*-$PMA(rChal)_{16}$ were prepared and consequently, four membranes were exposed to UV light (40 min) for complete crosslinking. Table 2 showed the data of crosslinked membranes with the block ratios of PEO_{11}-*b*-$PMA(rChal)_9$, PEO_{11}-*b*-$PMA(rChal)_{12}$ and PEO_{11}-*b*-$PMA(rChal)_{16}$ at different temperatures. It was clearly indicated that all of these block copolymers possessed same tendency with the block ratio of PEO_{11}-*b*-$PMA(rChal)_7$. At 60 °C, $\alpha_{CO2/N2}$ reached to 12.56 when the mole percentage of PMA (PMA%) was about 39%. Further, the $\alpha_{CO2/N2}$ reached to 14.79 when PMA% was approximately equal to 50%, however, the $\alpha_{CO2/N2}$ dropped to 10.13 when PMA% was greater than 60% (Fig. 4).

For solubility selectivities, the interactions between EO and CO_2 increased with rising the temperature. For diffusivity selectivities, the complicated crosslinking network led to the limited free volume. Moreover, crosslinking segments barely moved with the vary of temperature, so the N_2 denser barriers increased with the more crosslinking units[48]. When the ratio of PEO:PMA varied from 11:7 to 11:12, the N_2 permeabilities decreased as

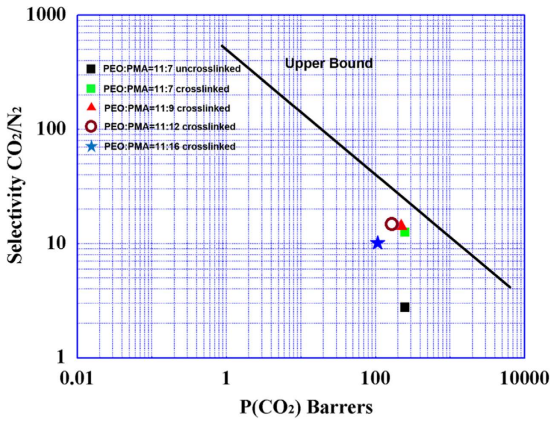

Figure 5. Robeson Upper Bound for CO_2/N_2 separation in 2008 with different block ratio copolymer membranes[53].

Temp(°C)	Crosslink Time (min)	N_2 Permeabilities (barrer)	CO_2 Permeabilities (barrer)	$\alpha_{(CO2/N2)}$
30	0	80.43	125.48	1.56
	5	46.24	119.31	2.58
	15	35.61	108.24	3.04
	40	29.05	100.53	3.46
60	0	97.78	237.62	2.43
	5	31.62	204.34	6.46
	15	17.21	176.84	10.28
	40	11.19	165.69	14.79

Table 3. Pure Gas Permeabilities and Selectivities of PEO-*b*-PMA(rChal) (11:12) Membrane under Different Crosslink Time. Permeances at 1×10^6 ($cm \cdot s^{-1} \cdot cmHg^{-1}$), were calculated by dividing the observed flow rate by the area of the membrane (2.84 cm^2) and the pressure gradient (10 psi) employed, using porous Al_2O_3 membrane supports. The values were obtained from 10 independent measurements and the mean value and standard deviations were determined. The error in each case was <5%. The membrane PEO-*b*-PMA (rChal) showed no difference of gas permeation in humid environment.

the data described. In contrast, CO_2 plasticized EO chain to be more flexible which resulted in higher CO_2/N_2 selectivities. However, the continuous increase of mole percentage of chalcone segments did not represent sustainable rising trend in $\alpha_{CO2/N2}$ but form a more rigid crosslinking framework instead. The rigid framework structure limited the mobility of EO segments in a large degree, which became obstacles for CO_2 transfer, representing a sharp reduction of $\alpha_{CO2/N2}$. As shown in Fig. 5, the highest CO_2 selectivities of crosslinked membranes in this work was much closer to upper bound[53] than un-crosslinked ones. Taking account of these factors, the content of crosslinking segments after fully crosslinking played a key role in CO_2 gas permeable membrane.

Comparison of CO_2 permeation properties of a fixed block ratio BCP under different irradiation time. For this study, the PEO_{11}-*b*-$PMA(rChal)_{12}$ was treated as an example. (The data for other membranes are shown in Tables S3 and S4). Chalcone was an unique UV-crosslinker because of its easy crosslinking degree control by altering the UV irradiation time, which provided us a feasible way to verify the mechanism that crosslinking degree affected the ultimate CO_2 permeation properties. Table 3 presented the system data obtained under different UV irradiation time 0 min, 5 min, 15 min and 40 min (fully crosslinked) at 30 °C and 60 °C, respectively. The observed results (Figure S2) revealed that the $\alpha_{CO2/N2}$ was rising with the variation of UV irradiation time. Specifically, the data of $\alpha_{CO2/N2}$ was 2.43 without UV irradiation at 60 °C and the $\alpha_{CO2/N2}$ reached to 6.46 after 5 min UV irradiation. Further, the $\alpha_{CO2/N2}$ value was reached to the maximum of 14.79 after 40 min of UV irradiation, which revealed the full crosslinking. With increasing the irradiation time, the crosslinking degree in chalcone units increased which were minimizing free volume of the framework, resulting in the decreasing of N_2 permeabilities. Meanwhile, harder crosslinked PMA segments may also be contributed to the improvement of CO_2/N_2 selectivities. For diffusivity selectivities, CO_2 would make EO chains more flexible in the limited area surrounded by the crosslinked wall, which caused high CO_2 permeabilities. On the other hand, the confinement of free volume would result in denser barriers as explained above, leading to the low N_2 permeabilities. Thus, based on the observed results, one can conclude that the demonstrated mechanism is fully consistent with the obtained results.

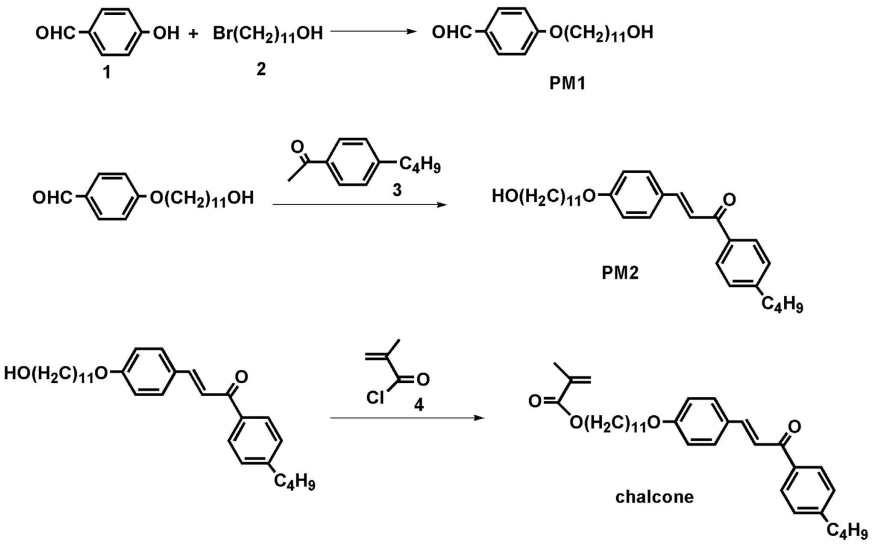

Figure 6. The synthesis route of chalcone.

Conclusion

In summary, we have successfully synthesized a series of diblock copolymers incorporating a novel UV-crosslinkable chalcone based on PEO chains using a facile RAFT process. Interestingly, it was observed that crosslinked membrane exhibited high CO_2 permeabilities over N_2 and hence showing high selectivities of CO_2, in contrast with un-crosslinked membrane. Further, the detailed studies revealed that the diblock copolymers with different proportion displayed various selectivities. It was researched that the rising amounts of chalcone within certain limits enhanced the crosslinking degree by which the EO fractions become more flexible and thus exhibiting a higher CO_2 permeabilities and selectivities with temperature enhancement. However, excess crosslinking chalcone fragment formed an ultra-rigid framework and confined the transfer of CO_2 through the membrane, which resulted in low CO_2 permeabilities. Thus, tunable CO_2 selectivities could be achieved by monitoring the crosslinking degree of membranes. The presented work provided further applications of UV-crosslinking network for CO_2 separation.

Materials and Methods

Materials. All the chemicals were analytical grade and used as received without any further purifications. 4-hydroxybenzaldehyde, Methoxypolyethylene glycols, 2-(Dodecyl- thiocarbonothioylthio)-2-methylpropionic acid (DDMAT), 11-bromoundecan-1-ol, Azo-bisisobutyronitrile (AIBN), Methacryloyl chloride, 4-butylphenylethylketone, N,N-Dimethylformamide (DMF), were all purchased from Sigma-Aldrich and Alfa-Aesar. Anisole was procured from Sigma-Aldrich with extra-dry grade purification.

Measurements. The prepared materials were characterized in detail using several techniques. The ^{1}H-NMR measurements were performed on Bruker AV-300 spectrometers in chloroform-d using tetramethylsilane (TMS; $\delta = 0$) as internal reference. All copolymers were examined by gel permeation chromatography (Malvern, GPC 270) as reported in our previous work[48]. The standard sample of GPC is Polystyrene(PS) and Mn = 99385, the measured solvent was THF. The DSC curve was measured in DSC(NETZSCH, STA449F3). Gas permeation measurements were carried out in the similar manner as reported in the literature by the authors; i.e. a home-made stainless steel permeation apparatus as described previously[21,48]. The UV-crosslinking of the films was monitored by UV-Vis absorption spectroscopy. The average thickness of the tested film was examined by ellipsometry. Six sections on each membrane were measured respectively to calculate the average thickness of $1.8 \pm 0.1\,\mu m$.

Synthesis of the monomer chalcone. The synthesis of monomer chalcone was done according to the Fig. 6 using organic synthetic procedure. The prepared material was purified with typical process and the purified product was characterized using ^{1}H-NMR spectroscopy.

Preparation of PM1. To prepare the PM1, in a typical reaction process, 4-hydroxybenzaldehyde (15.27 g, 125 mmol), 11-bromoundecan-1-ol (32.66 g, 125 mmol) and DMF (100 mL) were added in a 3-necked flask under continuous stirring. The mixture was stirred until the materials were completely dissolved. Consequently, 1.88 g NaI and 34.56 g K_2CO_3 were added in the resultant solution and stirred again for 30 min. After stirring, the resultant mixture was reflux for 24 h. After desired reaction time, the reaction was terminated and the mixture was cooled at room-temperature and the solvent was removed using rotary evaporation process. Subsequently, the residue was added to water and thus twice extracted with dichloromethane (DCM). Finally, the organic layer was separated and dried over $MgSO_4$ which was filtered. The obtained precipitate was then purified by column chromatography which finally provided a white solid (43.13 g). Yield: 90%. The ^{1}H NMR data measured in deuterochloroform ($CDCl_3$; 300 MHz) solvent exhibited several chemical shifts at δ 9.87 (1H, s), 7.84 (2H, d, J = 8.7 Hz), 6.99 (2H, d, J = 8.7 Hz), 4.03 (2H, t, J = 6.5 Hz), 3.64 (2H, t, J = 6.6 Hz), 1.81(2 H, m), 1.59–1.29 (12H, m). The

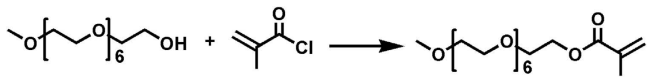

Figure 7. The synthesis route of EO precursor.

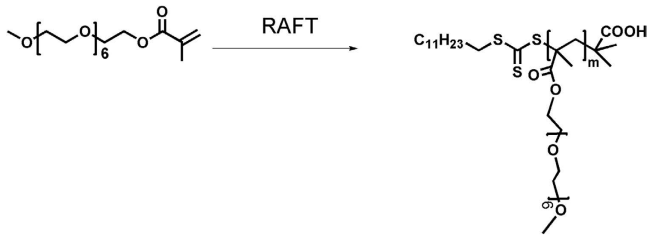

Figure 8. The synthesis route of PEO macro-initiators.

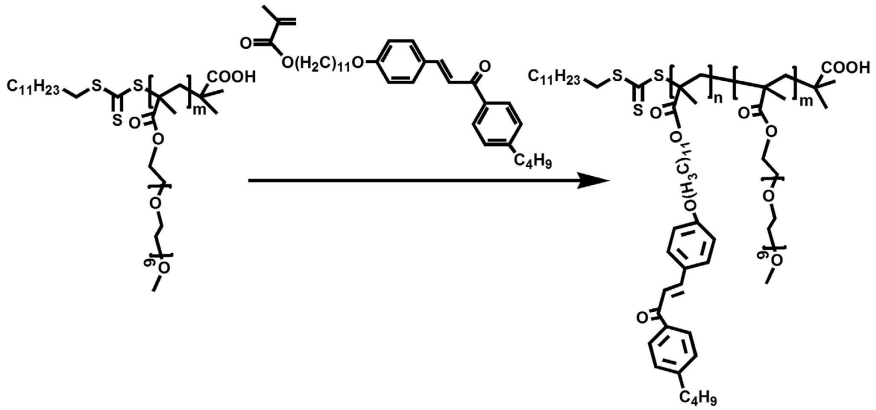

Figure 9. The synthesis route of PEO-*b*-PMA(rChal) (11:7, 11:9, 11:12, 11:16) diblock copolymers.

typical ^{1}H-NMR spectrum is shown in Figure S3. ^{13}C-NMR (400 MHz, $CDCl_3$, δ, ppm) 191.39, 164.26, 132.20, 129.73, 114.76, 77.15, 63.21, 32.92, 29.41, 26.28; TOF MS ($C_{18}H_{28}O_3$) *m/z:* calcd. for 292.410, found 293.212.

Preparation of PM2. To prepare PM2, in a typical process, PM1 (34.9 g, 100 mmol) and 3 namely, 4-butylphenylethylketone (21 g, 100 mmol) were mixed in alcoholic sodium hydroxide (50 mL, 10%) solution under continuous stirring. After 12 h stirring at room-temperature, the reaction mixture was poured into ice-water. The solid precipitate was formed which was collected by filtration and dried. The dried product was the further purified by column chromatography and finally yellow solid was obtained (50.31 g). Yield: 90%. The ^{1}H-NMR data measured in deuterochloroform ($CDCl_3$; 300 MHz) solvent exhibited several chemical shifts at δ (ppm): 7.90–7.81 (d, 4 H, phenyl proton), 7.76 (d, 1H) 7.31–7.28 (d, 2H, phenyl proton), 7.19 (d, 1 H), 7.00–6.97 (m, 2H, phenyl proton), 4.11 (t, 2H, CH_2O), 4.03 (t, 2H, CH_2O), 2.68 (t, 2H, CH_2Ph), 1.94 (s, 3H, CH_2, d, C(CH3)-), 1.82 (m, 2H, CH2), 1.70–1.31 (m, 20H, $(CH_2)_{10}$), 0.94 (t, 3 H, -$(CH_2)_3CH_3$) (Figure S4). ^{13}C-NMR (400 MHz, $CDCl_3$, δ, ppm) 190.32, 161.43, 148.23, 144.33, 136.37, 130.45, 128.72, 127.64, 120.00, 115.12, 77.17, 63.22, 35.71, 33.27, 32.81, 29.49, 25.75, 22.34, 13.90; TOF MS ($C_{30}H_{42}O_3$) *m/z:* calcd. for 453.310, found 453.227.

Preparation of chalcone. To prepare the chalcone, in a typical reaction process, PM2 (42.8 g, 115 mmol), TEA (1.82 ml, 120 mmol) and 100 ml DCM were added in a dry round-bottom flask. Consequently, methacryloyl chloride (14.57 ml, 115 mmol) was added dropwise to the mixture at 0 °C and the reaction was continued overnight. The obtained product was then added to the water and subsequently extracted with DCM twice. The organic layer was then separated and dried over $MgSO_4$. Finally, the obtained product was filtered and purified by column chromatography which gives a light yellow solid (40.66 g). Yield: ~95%. The ^{1}H-NMR data measured in deuterochloroform ($CDCl_3$; 300 MHz) solvent exhibited several chemical shifts at δ (ppm): 7.90–7.81 (d, 4H, phenyl proton), 7.76 (d, 1H), 7.31–7.28 (d, 2H, phenyl proton), 7.19 (d, v1H), 7.00–6.97 (m, 2H, phenyl proton), 6.10 (s, 1H, (H=C)), 5.54 (s, 1H, H=C)), 4.11 (t, 2H, CH_2O), 4.03 (t, 2H, CH_2O), 2.68 (t, 2H, CH_2Ph), 1.94 (s, 3H, CH_2, d, $C(CH_3)$-), 1.82 (m, 2H, CH_2), 1.70–1.31 (m, 20H, $(CH_2)_{10}$), 0.94 (t, 3H, -$(CH_2)_3CH_3$) (Figure S5). ^{13}C-NMR (400 MHz, $CDCl_3$, δ, ppm) 190.32, 167.66, 161.43, 148.25, 144.30, 136.28, 130.14, 128.62, 127.63, 125.08, 119.80, 114.84, 77.00, 68.30, 35.71, 33.33, 29.57, 25.97, 22.56, 18.31, 13.89; TOF MS ($C_{34}H_{46}O_4$) *m/z:* calcd. for 518.630, found 519.281.

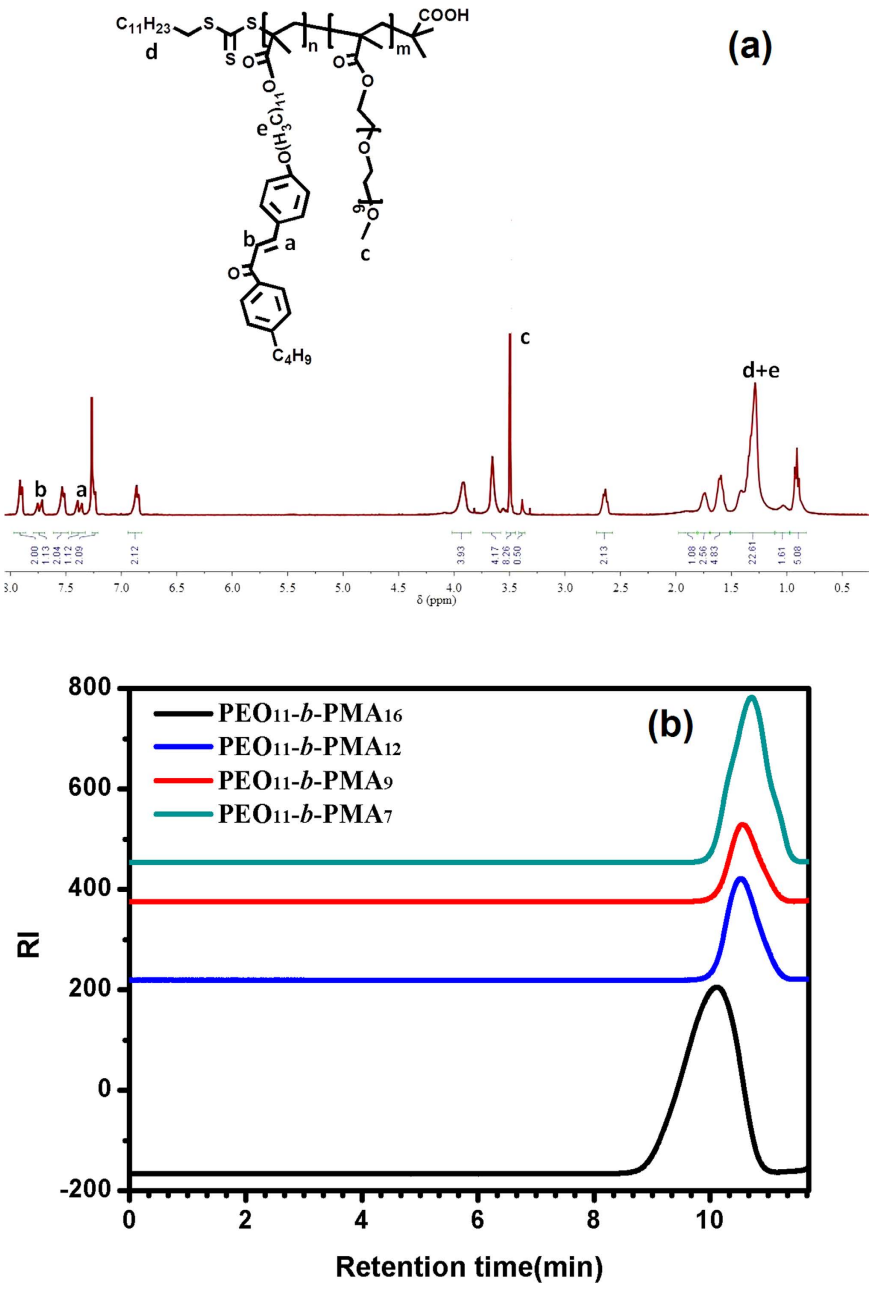

Figure 10. The ^{1}H-NMR and GPC of different block ratios of diblock copolymers.

Preparation of EO precursor. The synthesis of monomer was done according to the Fig. 7. In a typical synthesis process, solution of 10.5 g (100 mmol) methacryloyl chloride, in 30 mL DCM, was dropwise added to a mixture of 15.1 g (150 mmol) triethylamine and 35 g (100 mmol) methoxy polyethylene glycols (Mn = 350) in 100 mL of DCM at 0 °C. The resultant mixture was then stirred overnight. After overnight stirring, the resultant mixture was filtered and the obtained crude product was added to 100 ml water and subsequently extracted with DCM twice. Finally, the solvent was dried by rotary evaporation which leaves oily liquid (43.23 g). Yield: 95%. The ^{1}H-NMR data measured in deuterochloroform ($CDCl_3$; 300 MHz) solvent exhibited several chemical shifts at δ (ppm):1.93 (s, 3H), 3.24 (s, 3H), 3.54 (t, 24H, CH_2CH_2O), 3.65 (t, 2H), 4.32 (t, 2H), 5.58 (s, 1H, -C(CH_3)=CH_2), 6.15 (s, 1H, -C(CH_3)=CH_2).(Figure S6); ^{13}C-NMR (400 MHz, $CDCl_3$, δ, ppm) 167.32, 136.34, 125.56, 76.85, 70.50, 69.20, 63.55, 59.39, 18.31; TOF MS ($C_{20}H_{38}O_9$) *m/z*: calcd. for 422.510; found 422.277.

Preparation of PEO Macro-initiators. The macro-initiator was synthesized by the Reversible Addition-Fragmentation Chain Transfer Polymerization (RAFT) method. In a typical reaction process, 2.0 g (4.8 mmol) of EO precursor, 34.94 mg (0.096 mmol) of 2-(Dodecylthio-carbon-thioyl-thio)-2-methyl propionic acid (DDMAT) and 3.149 mg (0.0192 mmol) of Azobisisobutyro-nitrile (AIBN) were mixed in a 10 mL Shreck bottle with 1.5 ml anhydrous anisole. Consequently, the resultant mixture was degassed four times using the

freeze pump-thaw procedure and the bottle was sealed under vacuum. The sealed bottle was then placed in a preheated oil bath (90 °C) for 12 h. Finally, the solution was precipitated in hexane (Fig. 8). The obtained yield was 45.5% (0.91 mg). The observed Mn and PDI are 4600 and 1.13, respectively. The ^{1}H-NMR, measured in deutero-chloroform, exhibited several chemical shifts at δ (ppm):1.25–1.34 (t, 23H, -$C_{12}H_{23}$), 3.36–3.42 (s, 3H, -OCH_3) (Figure S7); ^{13}C-NMR (400 MHz, $CDCl_3$, δ, ppm) 216.01, 177.26, 174.59, 70.65, 68.34, 65.25, 52.46, 46.03, 43.37, 35.82, 33.37, 29.73, 29.62, 29.50, 29.27, 28.25, 26.23, 22.36, 13.94.

Preparation of PEO-*b*-PMA(rChal) diblock copolymers. A series of PEO-*b*-PMA(rChal) containing a chalcone mesogen with different content of polymerization were synthesized by RAFT method. The targeted material was prepared as presented in Fig. 9. As an example, a procedure to prepare PEO_{11}-*b*-$PMA(rChal)_7$ is described here. In a typical reaction process, 0.097 g (1 eqv) PEO macro-initiators, 0.24 g (30 eqv) chalcone and 0.0003 g (0.12 eqv) AIBN were mixed in a 10 mL Shreck bottle with 1.8 ml anhydrous anisole. Then, the mixture was degassed four times using the freeze pump-thaw procedure and sealed under vacuum. The sealed bottle was then placed in a preheated oil bath (90 °C) for 17 h. The solution was precipitated in diethyl ether and finally pure diblock copolymer was obtained. Figure 10 showed the typical ^{1}H-NMR (a) and GPC (b) results. The observed Mn and PDI of PEO_{11}-*b*-$PMA(rChal)_7$, PEO_{11}-*b*-$PMA(rChal)_9$, PEO_{11}-*b*-$PMA(rChal)_{12}$, PEO_{11}-*b*-$PMA(rChal)_{16}$ are 8200 and 1.13, 9200 and 1.11, 10800 and 1.16, 13200 and 1.19. The ^{1}H-NMR data measured in deuterochloroform ($CDCl_3$; 300 MHz) solvent exhibited several chemical shifts at δ (ppm):1.30–1.46 (t, 23H, -$C_{12}H_{23}$), 3.51–3.57 (s, 3H, -OCH_3), 1.19–1.23 (s, 22H, -$O(CH_2)_{11}O$-); ^{13}C-NMR (400 MHz, $CDCl_3$, δ, ppm) 208.61, 189.94, 177.90, 169.84, 164.89, 162.11, 148.52, 144.46, 136.15, 130.23, 128.69, 127.78, 115.09, 70.80, 68.31, 65.17, 35.77, 33.33, 29.63, 28.35, 26.18, 22.42, 14.13. The DSC curve of un-crosslinked block copolymer PEO_{11}-*b*-$PMA(rChal)_{12}$ was measured at a rate of 2 °C/min from 40 °C to 140 °C and shown in Figure S8.

Preparation of thin membranes. The diblock copolymer membrane was made by spin-coating (1000 rpm) of 6 wt% chloroform solutions on Anodic Alumina Oxide (AAO) substrate. The prepared diblock copolymer membrane was placed in vacuum for 4 h at room-temperature. Consequently, the crosslinking of the block copolymer membrane was exposed to UV light (365 nm) for a desirable time and finally the UV-crosslinked membrane was obtained.

Gas permeation measurements. A home-built gas permeation measurement system was used to estimate the gas permeation as described in our previous work[22,48]. The pure gases with different kinetic diameters such as N_2 and CO_2 were studied in this work. For this, a spin-coated membranes on AAO substrates were placed in the permeation cell with a support screen. The surface area of the tested membrane, available for gas transport, was estimated and found to be 2.84 cm^2. The membranes were placed in the test system cell to investigate the gas permeation test. The gases, after passing through the membrane in the cell, was directed into a glass U-tube flow meter (Acol = 0.03 cm^2) to give the volumetric flow rate of the gas. It was measured by recording the time (t) that was required for a liquid column to travel a distance (X_{column} = 10 cm). All the measurements were taken at ambient temperature and the values were obtained at steady-state (usually last for at least 2 h). The values were obtained from 10 independent measurements and the mean value and standard deviations were determined. The error in each case was <5%. The same experimental procedure was repeated for other targeted gas. In general, the permeation properties were sequentially measured for He, N_2 and CO_2, respectively. The permeance (P; 10^6 $cm{\cdot}s^{-1}{\cdot}cmHg^{-1}$) was calculated based on the equation (1)[48]:

$$P = \frac{X_{col} \cdot A_{col}}{t \cdot \frac{76p}{14.7} A_{mem}} \times 10^6. \quad (1)$$

And the selectivities (α) of gas A, over gas B, was defined based on the below equation (2)[48]:

$$\alpha_{A/B} = \frac{P_A}{P_B} \quad (2)$$

References

1. Sun, L. B. *et al.* Facile fabrication of cost-effective porous polymer networks for highly selective CO_2 capture. *J. Mater. Chem. A* **3,** 3252–3256, doi: 10.1039/C4TA06039C (2015).
2. Xu, Y. L. *et al.* Mimicking how plants control CO_2 influx: CO_2 activation of ion current rectification in nanochannels. *Npg Asia Mater.* **7,** e215, doi: 10.1038/am.2015.98 (2015).
3. Chen, Z. *et al.* Supramolecular fabrication of multilevel graphene-based gas sensors with high NO_2 sensibility. *Nanoscale* **7,** 10259–10266, doi: 10.1039/C5NR01770J (2015).
4. Tian, T. *et al.* Amidine-based fluorescent chemosensor with high applicability for detection of CO_2: a facile way to "see" CO_2. *Analyst* **138,** 991–994, doi: 10.1039/C2AN36401H (2013).
5. Liao, Y., Weber, J. & Faul, C. F. J. Fluorescent Microporous Polyimides Based on Perylene and Triazine for Highly CO_2-Selective Carbon Materials. *Macromolecules* **48,** 2064–2073, doi: 10.1021/ma501662r (2015).
6. Abel, B. A., Sims, M. B. & Mccormick, C. L. Tunable pH- and CO_2 -Responsive Sulfonamide-Containing Polymers by RAFT Polymerization. *Macromolecules* **48,** 5487–5495, doi: 10.1021/ma501662r (2015).
7. Lin, H. *et al.* CO_2-selective membranes for hydrogen production and CO_2 capture -Part I: Membrane development. *J. Membr. Sci.* **457,** 149–161,doi: 10.1016/j.memsci.2014.01.020 (2014).
8. Ramasubramanian, K., Zhao, Y. & Ho, W. S. W. CO_2 capture and H_2 purification: Prospects for CO_2 selective membrane processes. *Aiche. J.* **59,** 1033–1045, doi: 10.1002/aic.14078 (2013).
9. Hoang, V. T. & Serge, K. Predictive models for mixed-matrix membrane performance: a review. *Chem. Rev.* **113,** 4980–5028, doi: 10.1021/cr3003888 (2013).

10. Gin, D. L. & Noble, R. D. Designing the next generation of chemical separation membranes. *Science* **332,** 674–676, doi: 10.1126/science.1203771 (2011).
11. Wang, S. W., Chen, Z. & Wang, Y. The effect of the electric-field on the phase separation of semiconductor-insulator composite film. *Chem. Commun.* **51,** 765–767, doi: 10.1039/C4CC06353H (2015).
12. Yang, H. *et al.* Progress in carbon dioxide separation and capture: A review. *J. Environ. Sci.* **20,** 14–27, doi: 10.1016/S1001-0742(08)60002-9 (2008).
13. Hyo Won, K. *et al.* High-performance CO_2-philic graphene oxide membranes under wet-conditions. *Chem. Commun.* **50,** 13563–13566, doi: 10.1039/C4CC06207H (2014).
14. Wilfredo, Y., Anja, C., Jan, W. & Klaus-Viktor, P. Nanometric thin film membranes manufactured on square meter scale: ultra-thin films for CO_2 capture. *Nanotechnology* **21,** 395301–395307, doi: 10.1088/0957-4484/21/39/395301 (2010).
15. Dai, Z., Noble, R. D., Gin, D. L., Zhang, X. & Deng, L. Combination of Ionic liquids with membrane technology: A new approach for CO_2 separation. *J. Membr. Sci.* **497,** 1–20, doi: 10.1016/j.memsci.2015.08.060 (2016).
16. Thallapally, P. K. *et al.* Flexible (breathing) interpenetrated metal-organic frameworks for CO_2 separation applications. *J. Am. Chem. Soc.* **130,** 16842–16843, doi: 10.1021/ja806391k (2008).
17. Kita-Tokarczyk, K., Grumelard, J., Haefele, T. & Meier, W. Block copolymer vesicles—using concepts from polymer chemistry to mimic biomembranes. *Polymer* **46,** 3540–3563, doi: 10.1016/j.polymer.2005.02.083 (2005).
18. Yilgör, I. & Yilgör, E. Hydrophilic polyurethaneurea membranes: influence of soft block composition on the water vapor permeation rates. *Polymer* **40,** 5575–5581, doi: 10.1016/S0032-3861(98)00766-6 (1999).
19. Xia, J., Liu, S. & Chung, T. S. Effect of End Groups and Grafting on the CO_2 Separation Performance of Poly(ethylene glycol) Based Membranes. *Macromolecules* **44,** 7727–7736, doi: 10.1021/ma201844y (2011).
20. Lin, H. & Freeman, B. D. Materials selection guidelines for membranes that remove CO_2 from gas mixtures. *J. Mol. Struct.* **739,** 57–74, doi: 10.1016/j.molstruc.2004.07.045 (2005).
21. Wang, Y. *et al.* Fabrication of CO_2 Facilitated Transport Channels in Block Copolymer through Supramolecular Assembly. *Polymers* **6,** 1403–1413, doi: 10.3390/polym6051403 (2014).
22. Li, X., Tian, T., Leolukman, M., Wang, Y. & Jiang, L. A Supramolecular Approach to Probing the Influence of Micro-Phase Structure on Gas Permeability of Block Copolymer Membranes. *Sci. Adv. Mater.* **5,** 719–726, doi: 10.1166/sam.2013.1591 (2013).
23. Wang, Y., Janout, V. & Regen, S. L. Creating Poly(ethylene oxide)-Based Polyelectrolytes for Thin Film Construction Using an Ionic Linker Strategy. *Chem. Mater.* **22,** 1285–1287, doi: 10.1021/cm9035488 (2010).
24. Anne-Valérie, R. & Ludwik, L. Block copolymers in tomorrow's plastics. *Nat. Mater.* **4,** 19–31, doi: 10.1038/nmat1295 (2012).
25. Li, M. & Ober, C. K. Block copolymer patterns and templates. *Mater. Today* **9,** 30–39, doi: 10.1016/S1369-7021(06)71620-0 (2006).
26. Zhang, Q., Wang, W. J., Lu, Y., Li, B. G. & Zhu, S. Reversibly Coagulatable and Redispersible Polystyrene Latex Prepared by Emulsion Polymerization of Styrene Containing Switchable Amidine. *Macromolecules* **44,** 6539–6545, doi: 10.1021/ma201056g (2011).
27. Yan, Q. *et al.* CO_2-responsive polymeric vesicles that breathe. *Angew. Chem. Int. Edit* **50,** 4923–4927, doi: 10.1002/anie.201100708 (2011).
28. Yu, T., Yamada, T., Gaviola, G. C. & Weiss, R. G. Carbon Dioxide and Molecular Nitrogen as Switches between Ionic and Uncharged Room-Temperature Liquids Comprised of Amidines and Chiral Amino Alcohols. *Chem. Mater.* **20,** 5337–5344, doi: 10.1021/cm801169c (2008).
29. Chen, X., Wang, Y. & Jiang, L. Research Progress of Preparation Methods of CO_2-Favored Permeation Membranes. *Chem. J. Chinese. Univers.* **34,** 249–268, doi: 10.7503/cjcu20120247 (2013).
30. Metz, S. J., Mulder, M. H. V. & Wessling, M. Gas-Permeation Properties of Poly(ethylene oxide) Poly(butylene terephthalate) Block Copolymers. *Macromolecules* **37,** 4590–4597, doi: 10.1021/ma049847w (2004).
31. Car, A., Stropnik, C., Yave, W. & Peinemann, K. V. Pebax®/polyethylene glycol blend thin film composite membranes for CO_2 separation: Performance with mixed gases. *Sep. Purif. Technol.* **62,** 110–117, doi: 10.1016/j.seppur.2008.01.001 (2008).
32. Anja, C., Chrtomir, S., Wilfredo, Y. & Klaus-Viktor, P. Tailor made Polymeric Membranes based on Segmented Block Copolymers for CO_2 Separation. *Adv. Func. Mater.* **18,** 2815–2823, doi: 10.1002/adfm.200800436 (2008).
33. Husken, D., Visser, T., Wessling, M. & Gaymans, R. J. CO_2 permeation properties of poly(ethylene oxide)-based segmented block copolymers. *J. Membr. Sci.* **346,** 194–201, doi: 10.1016/j.memsci.2009.09.034 (2010).
34. Kashimura, Y., Aoyama, S. & Kawakami, H. Gas Transport Properties of Asymmetric Block Copolyimide Membranes. *Polym. J.* **41,** 961–967, doi: 10.1295/polymj.PJ2009108 (2009).
35. Reijerkerk, S. R., Arun, A., Gaymans, R. J., Nijmeijer, K. & Wessling, M. Tuning of mass transport properties of multi-block copolymers for CO_2 capture applications. *J. Membr. Sci.* **359,** 54–63, doi: 10.1016/j.memsci.2009.09.045 (2010).
36. Zhao, H. Y., Cao, Y. M., Ding, X. L., Zhou, M. Q. & Quan, Y. Effects of cross-linkers with different molecular weights in cross-linked Matrimid 5218 and test temperature on gas transport properties. *J. Membr. Sci.* **323,** 176–184, doi: 10.1016/j.memsci.2008.06.026 (2008).
37. Lin, H., Bd, V. W. E., Toy, L. G. & Gupta, R. P. Plasticization-enhanced hydrogen purification using polymeric membranes. *Science* **311,** 639–642, doi: 10.1126/science.1118079 (2006).
38. Car, A., Yave, W., Peinemann, K.-V. & Stropnik, C. Tailoring Polymeric Membrane Based on Segmented Block Copolymers for CO_2 Separation, in Membrane Gas Separation (eds Yampolskii, Y. & Freeman, B.), John Wiley & Sons, Ltd, Chichester, UK Chapter 12, 227–253, doi: 10.1002/9780470665626.ch12(2010).
39. Lin, H., Kai, T., Freeman, B. D., Kalakkunnath, S. & Kalika, D. S. The Effect of Cross-Linking on Gas Permeability in Cross-Linked Poly(Ethylene Glycol Diacrylate). *Macromolecules* **38,** 8381–8393, doi: 10.1021/ma0510136 (2005).
40. Espuche, E., Escoubes, M., Cuney, S. & Pascault, J. P. Gas permeability of model polyurethane networks and hybrid organic-inorganic materials: Relations with morphology. *J. Appl. Polym. Sci.* **65,** 2579–2587, doi: 10.1002/(SICI)1097-4628(19970919)65:12 (1997).
41. Yave, W., Car, A., Funari, S. S., Nunes, S. P. & Peinemann, K. V. CO_2-Philic Polymer Membrane with Extremely High Separation Performance. *Macromolecules* **43,** 326–333, doi: 10.1021/ma901950u (2009).
42. Japip, S., Liao, K. S., Xiao, Y. & Chung, T. S. Enhancement of molecular-sieving properties by constructing surface nano-metric layer via vapor cross-linking. *J. Membr. Sci.* **497,** 248–258, doi: 10.1016/j.memsci.2015.09.045 (2015).
43. Ma, C. *et al.* Thin-skinned intrinsically defect-free asymmetric mono-esterified hollow fiber precursors for crosslinkable polyimide gas separation membranes. *J. Membr. Sci.* **493,** 252–262, doi: 10.1016/j.memsci.2015.06.018 (2015).
44. Zhao, H. *et al.* A novel multi-armed and star-like poly (ethylene oxide) membrane for CO_2 separation. *J. Membr. Sci.* **489,** 258–263, doi: 10.1016/j.memsci.2015.04.028 (2015).
45. Kammakakam, I., Yoon, H. W., Nam, S. Y., Park, H. B. & Kim, T. H. Novel piperazinium-mediated crosslinked polyimide membranes for High performance CO_2 separation. *J. Membr. Sci.* **487,** 90–98, doi: 10.1016/j.memsci.2015.03.053 (2015).
46. Kusuma, V. A. *et al.* Crosslinked poly (ethylene oxide) containing siloxanes fabricated through thiol-ene photochemistry. *J. Polym. Sci. Part A: Polym. Chem.* **53,** 1548–1557, doi: 10.1002/pola.27594 (2015).
47. Scofield, J. M. *et al.* High-performance thin film composite membranes with well-defined poly (dimethylsiloxane)-*b*-poly (ethylene glycol) copolymer additives for CO_2 separation. *J. Polym. Sci. Part A: Polym. Chem.* **53,** 1500–1511, doi: 10.1002/pola.27628 (2015).
48. Xue, B. *et al.* CO_2-selective free-standing membrane by self-assembly of a UV-crosslinkable diblock copolymer. *J. Mater. Chem* **22,** 10918–10923, doi: 10.1039/C2JM31037F (2012).

49. Miyatake, M., Kimura, T., Komiyama, H., Komura, M. & Iyoda, T. Large-area Fabrication of Free-Standing Thick Membrane with Microphase-Separated Cylindrical Nanostructure. *Trans. Mater. Res. Soc. Japan*. **37,** 409–412, doi: 10.14723/tmrsj.37.409 (2012).
50. Tian, Y., Watanabe, K., Kong, X., Abe, J. & Iyoda, T. Synthesis, Nanostructures, And Functionality Of Amphiphilic Liquid Crystalline Block Copolymers With Azobenzene Moieties. *Macromolecules* **35,** 3739–3747, doi: 10.1021/ma011859j (2002).
51. Tian, Y., Kong, X., Nagase, Y. & Iyoda, T. Photocrosslinkable liquid-crystalline block copolymers with coumarin units synthesized with atom transfer radical polymerization. *Polym. Sci. Part A: Polym. Chem*. **41,** 2197–2206, doi: 10.1002/pola.10767 (2003).
52. Rahman, M. M. *et al.* Influence of Poly(ethylene glycol) Segment Length on CO_2 Permeation and Stability of PolyActive Membranes and Their Nanocomposites with PEG POSS. *Acs Appl. Mater. Inter.* **7,** 12971–12978, doi: 10.1021/am504223f (2014).
53. Robeson, L. M. The upper bound revisited. *J. Membr. Sci*. **320,** 390–400, doi: 10.1016/j.memsci.2008.04.030 (2008).

Acknowledgements

This work was supported by National Natural Science Foundation of China (Grant No. 51373005, 51673007), National Key Basic Research Program of China (2014CB931800), Program for New Century Excellent Talents in University (NCET-10-0035) and Fundamental Research Funds for the Central Universities.

Author Contributions

J.L. and Y.W. initiated and designed entire project. J.L., Z.C., Y.S., X.Z. participated in the experiments and Y.L. supported the study. J.L., Y.W. and A.U. prepared and checked the manuscript. Y.W. conceived the research project and directed the study. All the authors reviewed the manuscript.

Additional Information

Supplementary information accompanies this paper at http://www.nature.com/srep

Competing financial interests: The authors declare no competing financial interests.

How to cite this article: Li, J. *et al.* Probe Into the Influence of Crosslinking on CO_2 Permeation of Membranes. *Sci. Rep.* **7**, 40082; doi: 10.1038/srep40082 (2017).

Publisher's note: Springer Nature remains neutral with regard to jurisdictional claims in published maps and institutional affiliations.